

*functional
genomics*



accelerated drug
discovery

Union Biometrika N.V.

European Scientific Operations

a Harvard Biosciences company

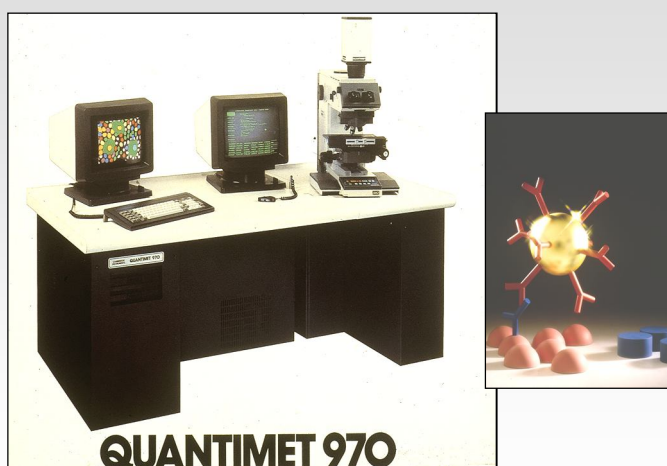
The Eazyx Imaging System
Exploring Dimensions

January 2004

History

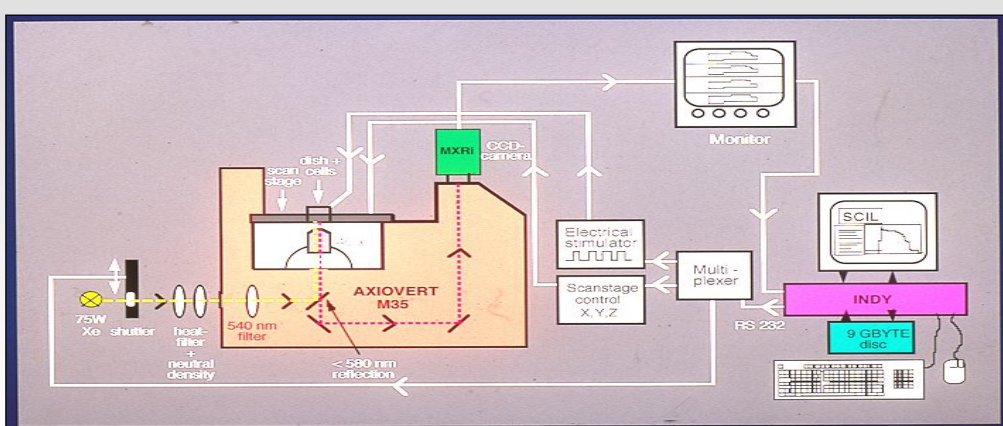
Software and Hardware
Nanovid Microscopy
MIAS-1
SCIL Image 1.x – eaZYX 1

Nanovid Microscopy - Immunogold 1985



Quantimet 970 -1983
Nanovid microscopy, VEDIC, 20 nm resolution, immunogold labeling - 1985

MIAS-1 1993



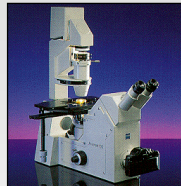
Imaging setup for stimulation studies of isolated cardiomyocytes in 1993
 Ca^{2+} ratio-imaging real-time acquisition (10 msec) and analysis.

Picture courtesy of J&J PRD

MIAS-1 2001



SGI Unix Workstation
for image acquisition control
and image analysis



Carl Zeiss Axiovert 135
microscope



Intensified camera
low-light, high speed



Cell Biology Setup



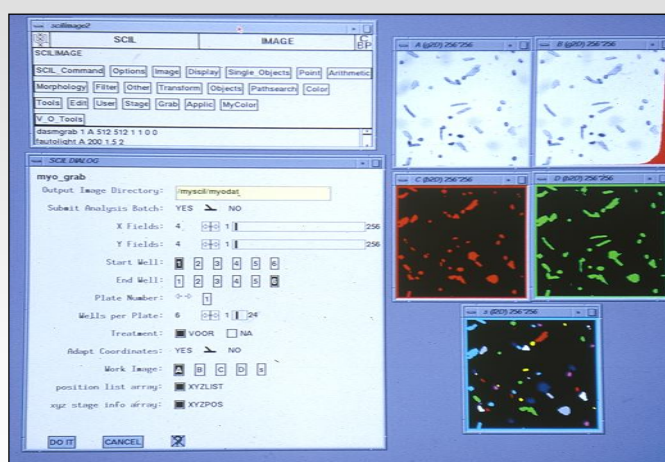
In Vivo Cell Biology Setup



Tissue Morphology Setup

Pictures courtesy of J&J PRD

SCIL Image 1993 - 2001



SCIL Image 1.3 on Silicon Graphics Unix Indy Workstation

Pictures courtesy of J&J PRD

MIAS-2™ & eaZYX™

Exploring dimensions
Software and Hardware

MIAS-2™ & eaZYX™

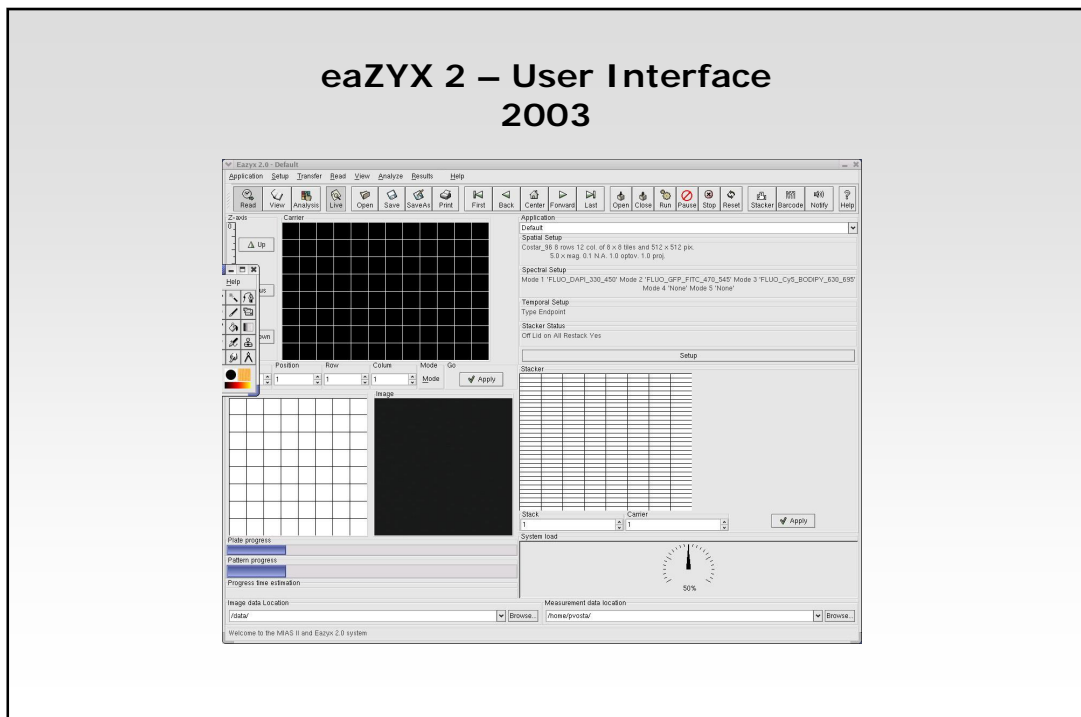
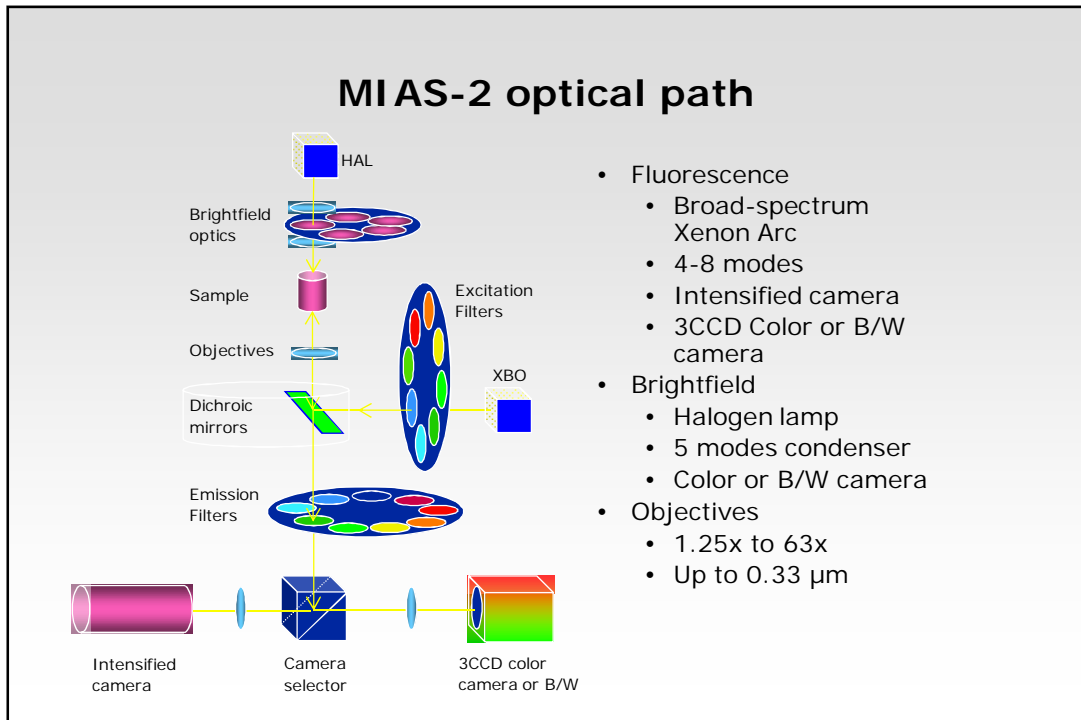
2003



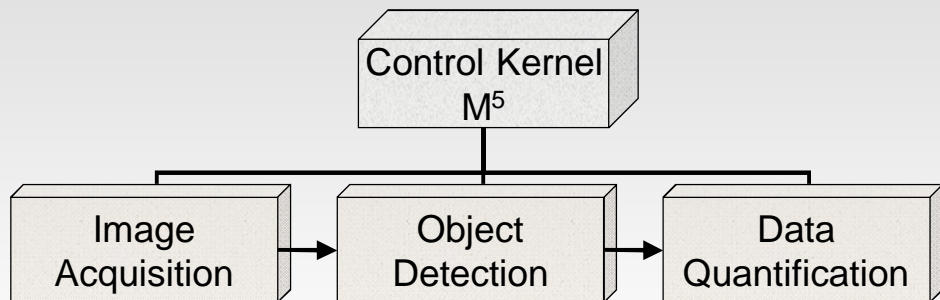
Features

Explore XY(Z), λ , t

- Spatial
 - Multiple carriers (SBS-standard)
 - Tiles N x N (x N)
- Spectral
 - Fluorescence
 - Ultra low light
 - Intensified camera
 - Autofocus
 - Brightfield
 - B/W or color camera
- Temporal
 - Video
 - Time-lapse
- Automation
 - Plate stacker
 - Barcode
 - System Integration

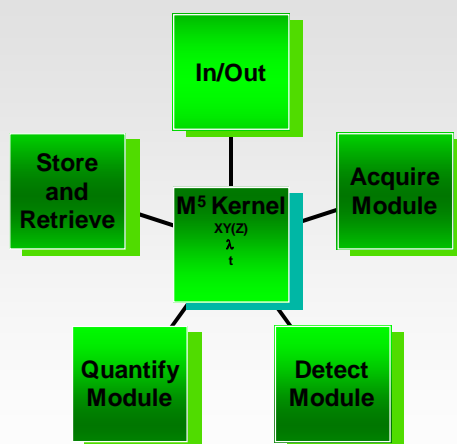


eaZYX 2 from Image to Data



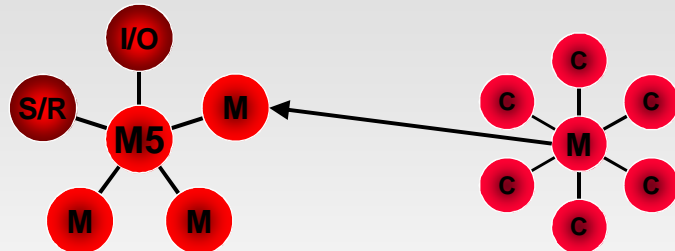
Flow management framework

eaZYX 2 M⁵ Control Kernel



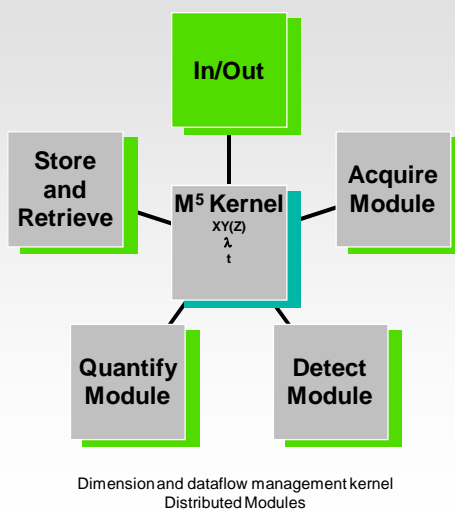
Dimension and dataflow management kernel
Distributed Modules

eaZYX 2 M⁵ Control Kernel Hierarchy of Integration



- Stepwise and modular integration
 - Modules (M)
 - Components (C)
- Integrated or distributed
- CORBA for communication (open standard)
- ANSI C and C++ (preferred)

In/Out Communication



In/Out Communication- Visual

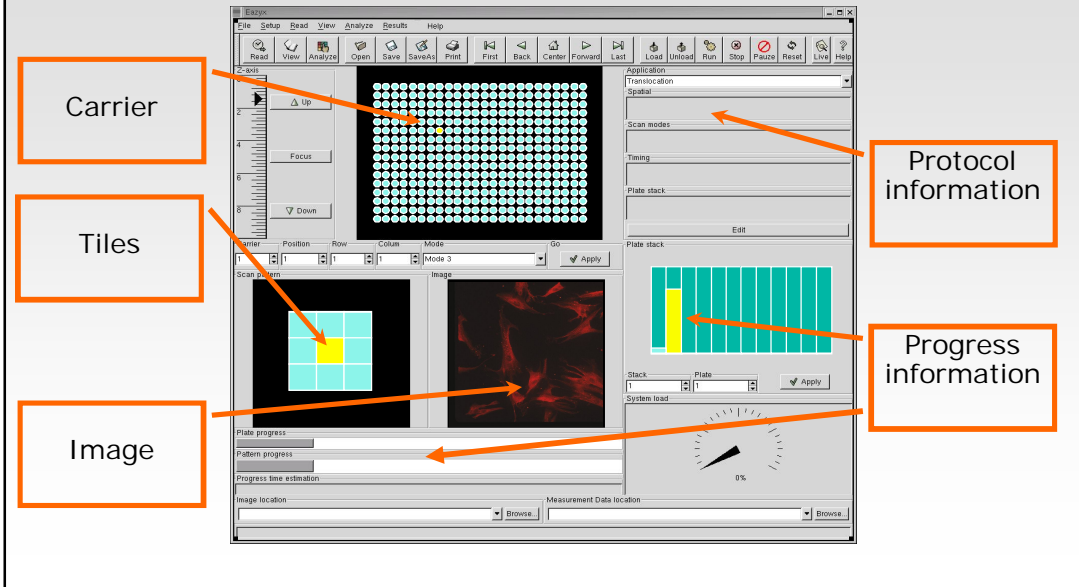
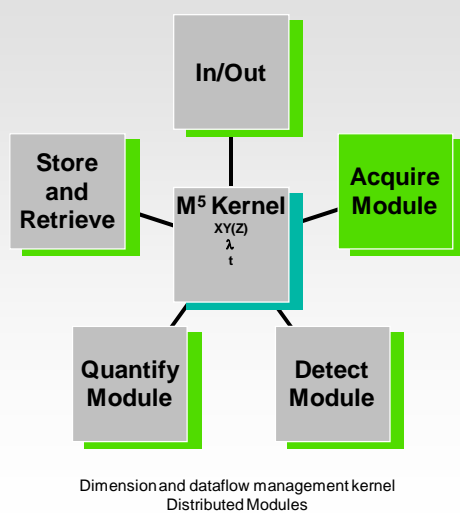
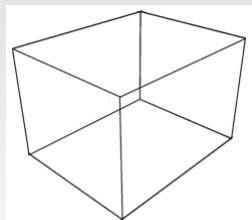


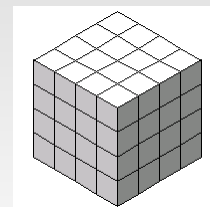
Image Acquisition



Spatial Exploration – 3D Space



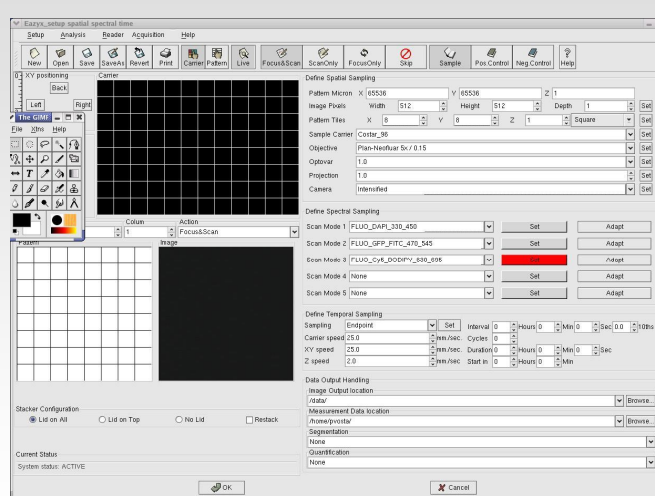
Outer limits



Inner limits

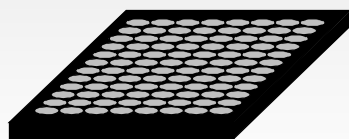
A Cartesian (XYZ) coordinate system defines the space which can be explored with the instrument

Spatial Spectral and Temporal

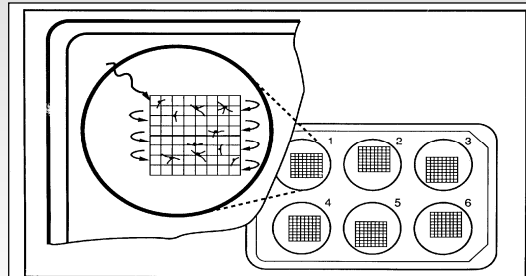


Defining M⁵ kernel settings

Spatial Tiled Image Acquisition



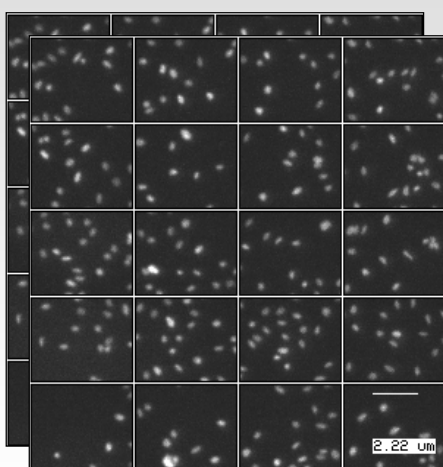
Pattern location



Tiled pattern

Automated tiled scanning principle in 2D
A two step scanning principle – a coarse grid with fine tileing

Spatial – Square Tile Pattern Nuclear Localization Screening (NLS)



Rectangular 4x5 image mosaic - view on one well

- Hoechst stained nuclei of E11 synovial fibroblasts
 - 40x magnification, 60 wells
 - 4 x 5 tiled mosaic scanned
 - 693 x 513 pixels / image
 - 2772 x 2656 pix. / mosaic
- Focus 1x in each well
- 15 min. per plate x 2

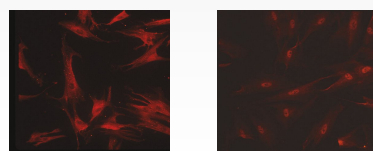
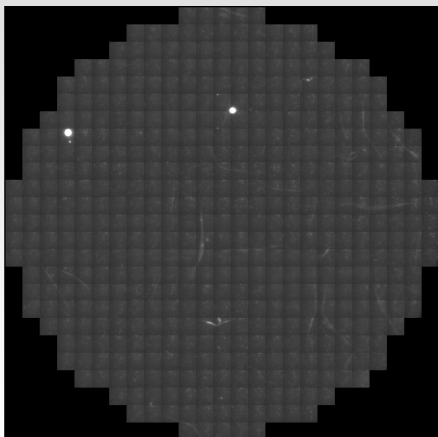


Image courtesy of J&J PRD

Spatial - Circular Tile Pattern *C. elegans*



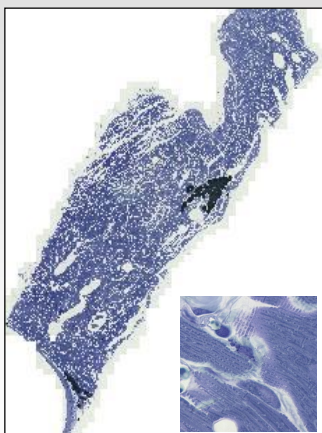
- Central 60 wells of 96 well plate
 - 40x magnification (dry)
 - 473 512x512 pixel images / well
 - 20x focus / well (1200x / plate)
 - 28380 images in less than 4 hours
 - 0.5 seconds / image including travel
 - Mosaic of 12800 x 12800 pixels



Circular tiled mosaic scanned - view on one well

Images courtesy of J&J PRD

Spatial - Dynamic Tile Pattern

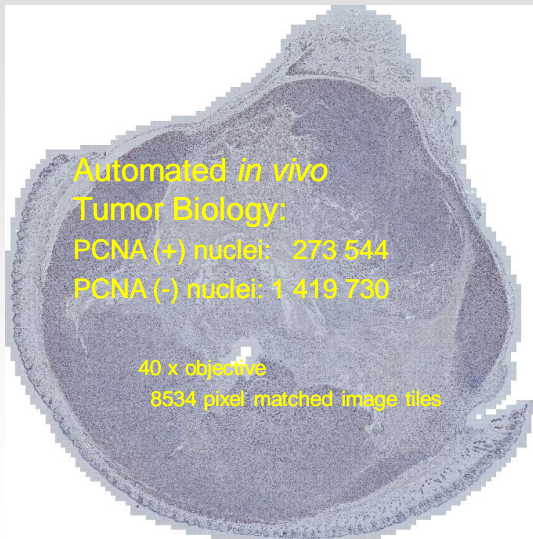


Tissue scan on ZEISS Axiophot
SONY 950P 3CCD RGB color camera

- Toluidin blue stained rabbit heart tissue, Epon 2 μ semi thin slice
 - 63x, immersion oil
 - 1300 512x512 images (0.75 Gb TIFF)
 - 433x auto focus
 - 40 minutes scan for complete mosaic
 - 51x66=3366 image tiles
 - 26112 x 33792 pixels (1.9 Gb)
 - Automated tissue edge detection by software

Image courtesy of J&J PRD

Spatial - Dynamic Tile Pattern

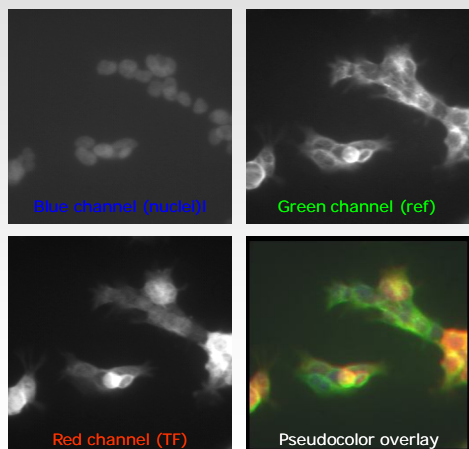


- Random selection of area's caused variability
- Automated whole tissue analysis provides *all* data for a section
- Reduced hands-on time (2 min.)

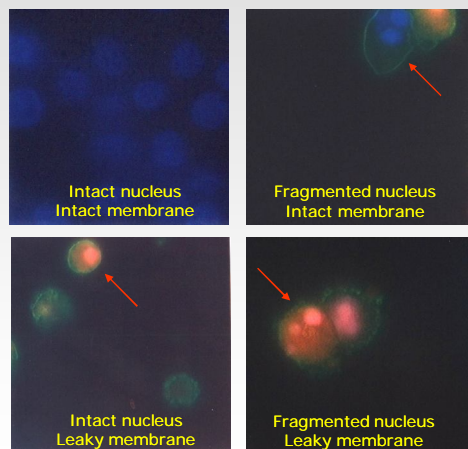
Tumor proliferation by PCNA-positive nuclei
DAB immunocytochemistry

Spectral Multispectral Acquisition

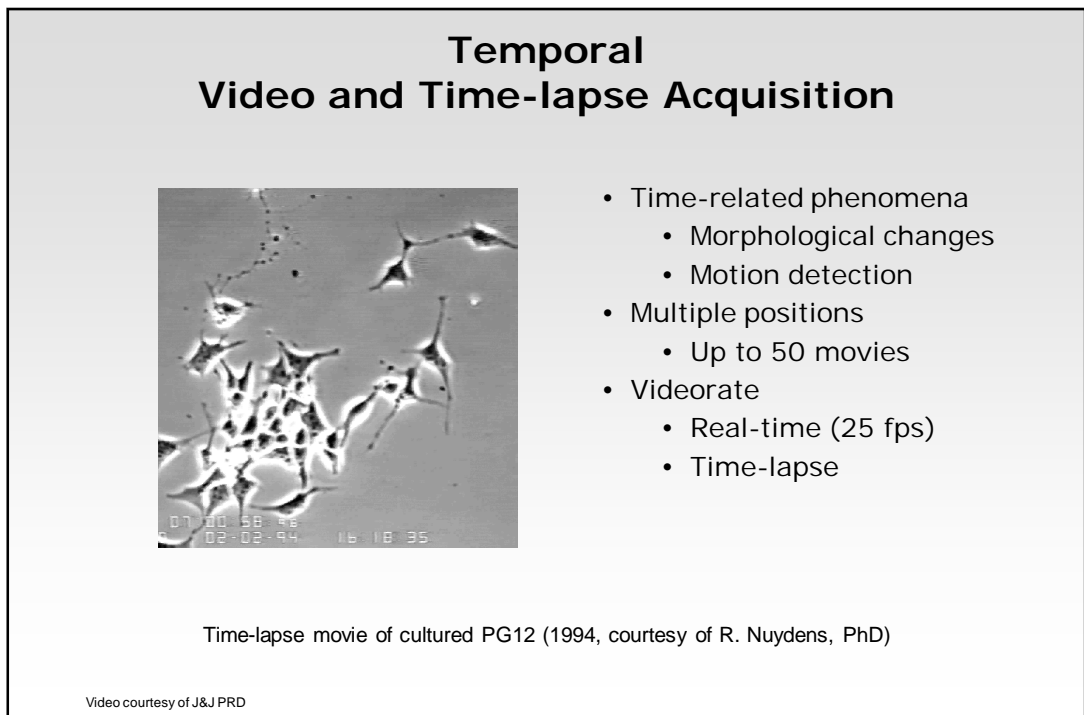
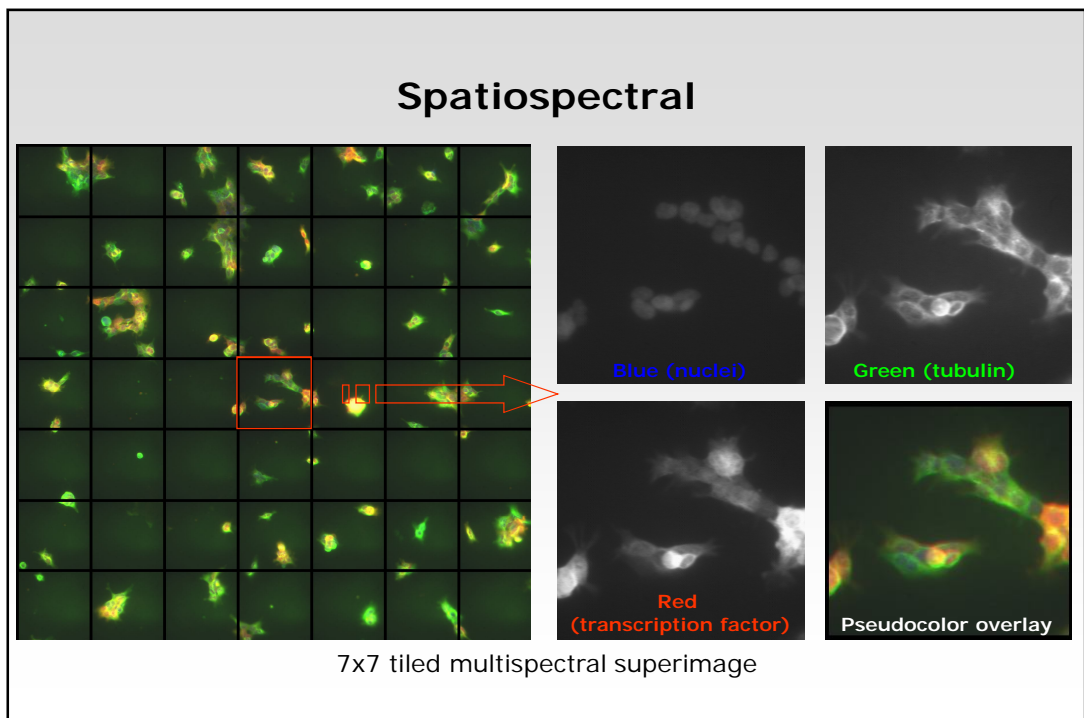
Expression / Translocation



Apoptosis



Pixel-matched images of 1 to 5 different emission wavelengths

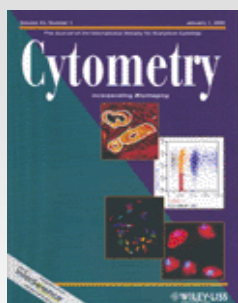


Finding the Sample A Robust Autofocus System

- Need for robust general purpose autofocus system
- Fluorescence, bright field microscopy and phase contrast
- Reliable (>99%) at all magnifications (5x, ..., 40x, 63x)
- Insensitive to noise in fluorescence microscopy
- High speed, video rate implementation
- Large scale unattended operation possible

Robust Autofocusing in Microscopy, Jan-Mark Geusebroek et al., Cytometry 39:1-9 (2000)

A robust auto-focus algorithm



Robust autofocusing in microscopy

Jan-Mark Geusebroek ^{1,2*}, Frans Cornelissen ²,
Arnold W.M. Smeulders ¹, Hugo Geerts ²

¹Department of Computer Science, Faculty of Science, University of Amsterdam, Amsterdam, The Netherlands

²Life Sciences, Janssen Research Foundation, Beerse, Belgium

Cytometry, 2000, **39**: 1-9 & Pat. WO / 0075709

- Content-based auto-focus system
 - Min. 300 msec. (5 frames)
 - Robust in extreme low light conditions
 - Robust in low S.N.R. conditions

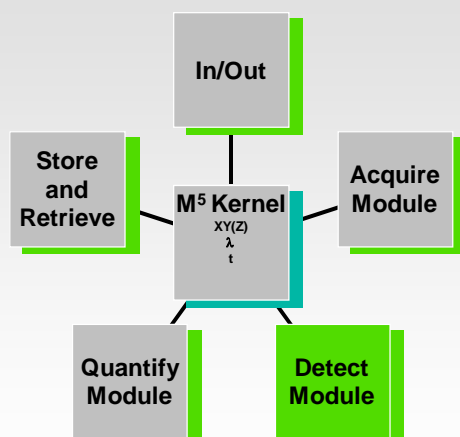
Autofocus and Scanning at Work Low light conditions



Nuclear Localisation Screening (NLS)
Image acquisition

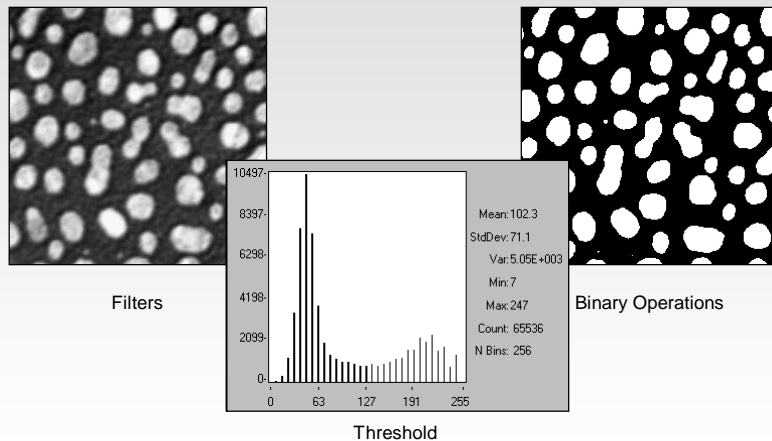
Video courtesy of J&J PRD

Object Detection



Dimension and dataflow management kernel
Distributed Modules

Conventional Image Processing Filters and Thresholds



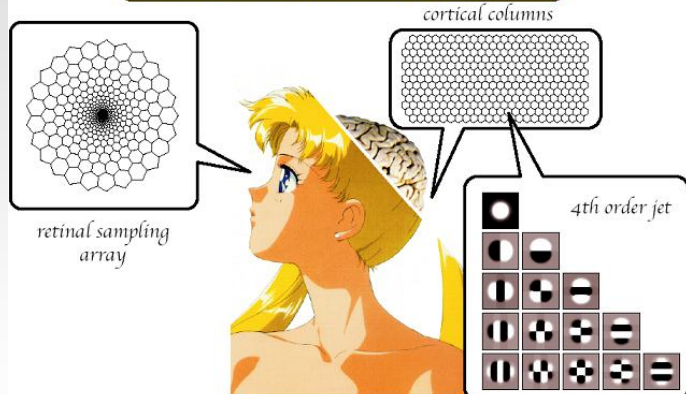
Threshold on gray value of 128 - bright foreground versus dark background

Scale Space

Frontend Vision
Gaussian Scale Space

The Visual System as a Geometry Engine

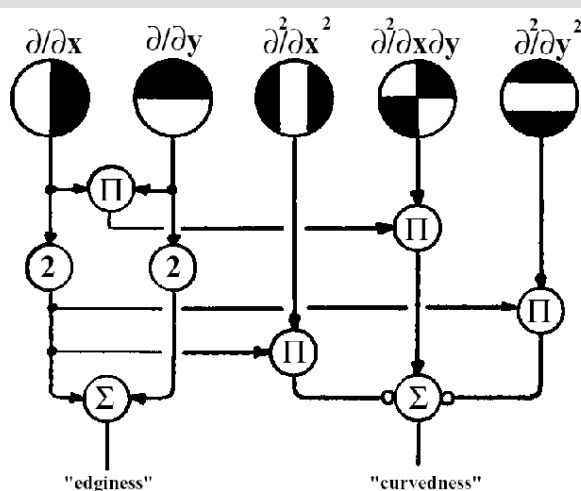
The visual system: A "geometry engine", booting up topology ("local sign"), implementing multiscale differential geometry (the "local jets"), etc., ...



Geometry and scale

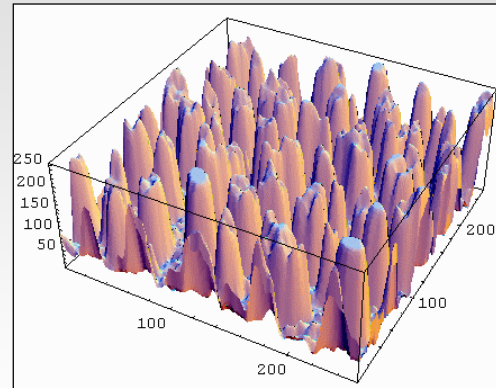
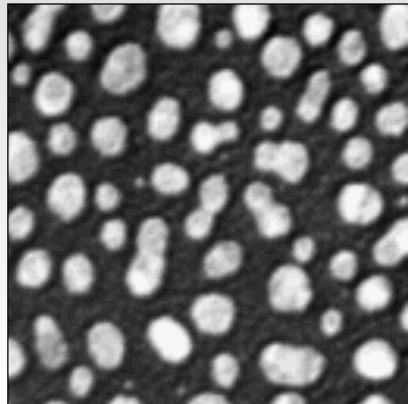
Courtesy of Jan Koenderink

Analyzing Geometry



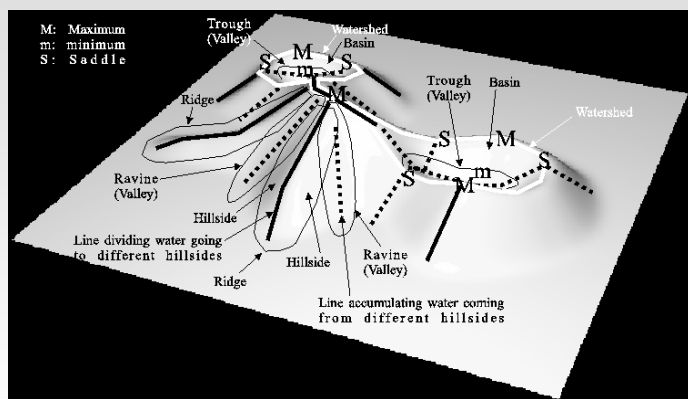
Courtesy of Jan Koenderink

Differential Geometry Shape and Scale



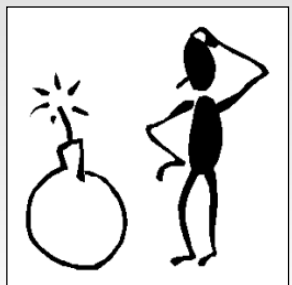
A 2D grayscale image landscape with gray value intensity seen as a 3D landscape

Geometric Patterns

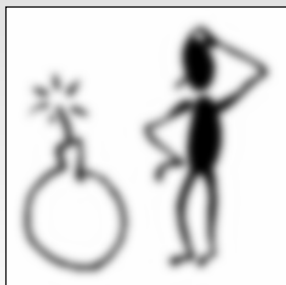


Geometric patterns in an image
Describe shape with differential geometry

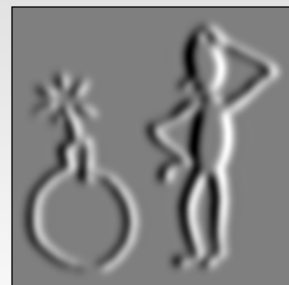
Differentiation with a Gaussian kernel



Original 256x256 pixels image
(L)



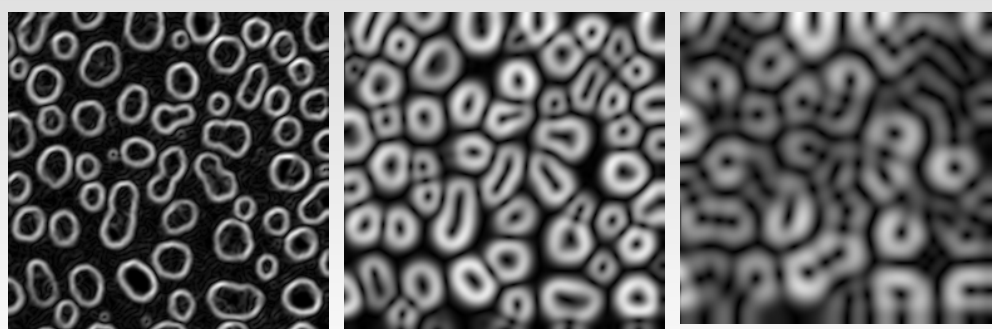
Zero order Gaussian
just blurring



First order Gaussian
 x -derivative (L_x)

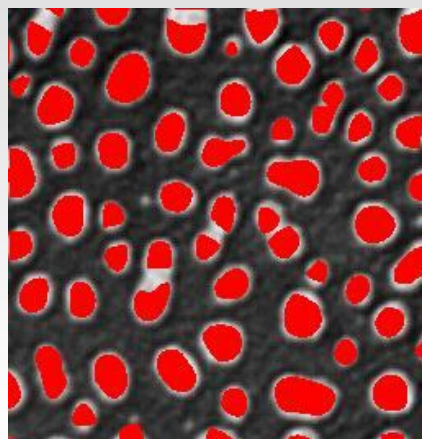
Differentiating a 2D image by convolution with the derivative of a Gaussian kernel

Gaussian Scale Selection

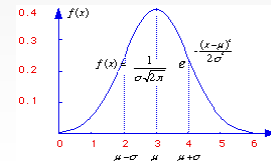


Intensity gradient L_w at scale (σ) 1, 5 and 10
camera noise elimination and size selection

Differential Geometry and Scale Elliptic Patch Detection



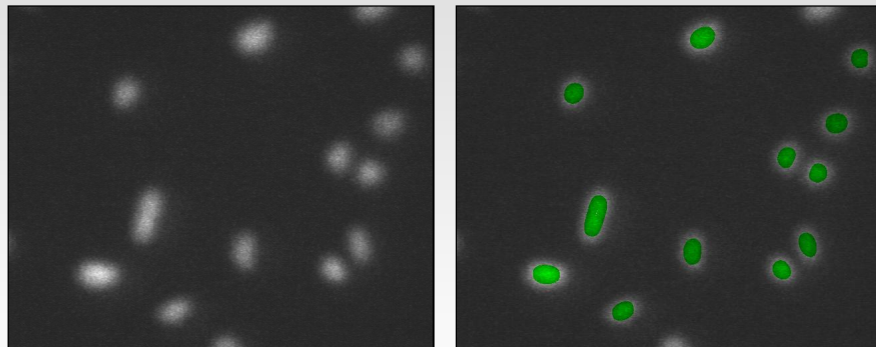
- Detecting bright elliptic regions on a dark background
- Object size selection with σ of Gaussian convolution kernel
- det. Hessian = $|H_f| = f_{xx}f_{yy} - f_{xy}^2$
 - deviation of flatness: magnitude and direction
- $f_{xx} < 0$ and $f_{xx}f_{yy} - f_{xy}^2 > 0$
- $L_{xx} < 0$ and $L_{xx}L_{yy} - L_{xy}^2 > 0$
- $L_{ww} < 0$ and $L_{vv}L_{ww} - L_{vw}^2 > 0$



Scale Space Applications

Shape
Scale

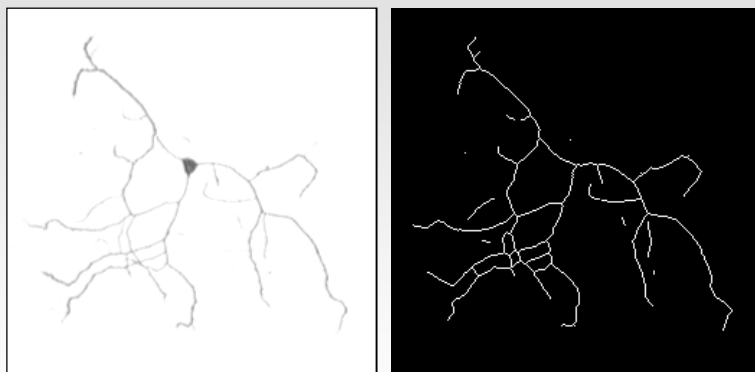
Elliptic patch Nuclear Localisation Screen



Processing noisy images
 $L_{xx} < -0.0004$ and $L_{xx}L_{yy} - L_{xy}^2 > 0$, scale sigma (σ) 9.0
40x, Hoechst stained nuclei, Photonic Science ISIS-3 intensified CCD camera

Image courtesy of J&J PRD

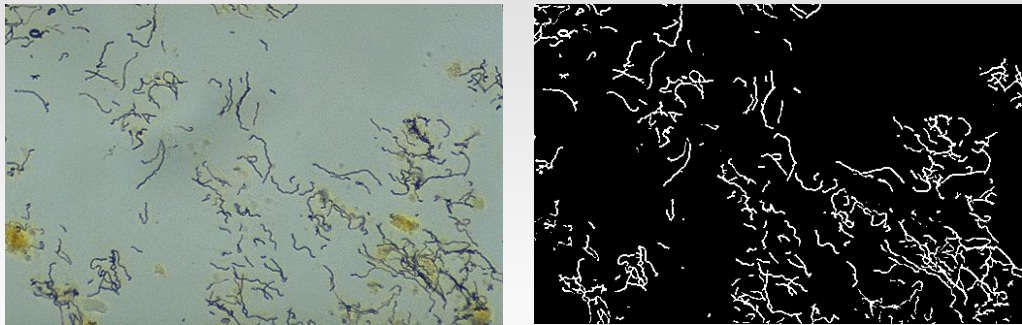
Ridge Line detection in Neurite Tracking



A line detector for dark ridges on an uneven background
 $L_{xx}L_{yy} - 2L_{xy}L_{xy} + L_{yy}L_{xx}$ or $L_{pp} > 4.0 * \text{threshold} / \sigma^2$
Scale (σ) 2.0, threshold 1.0

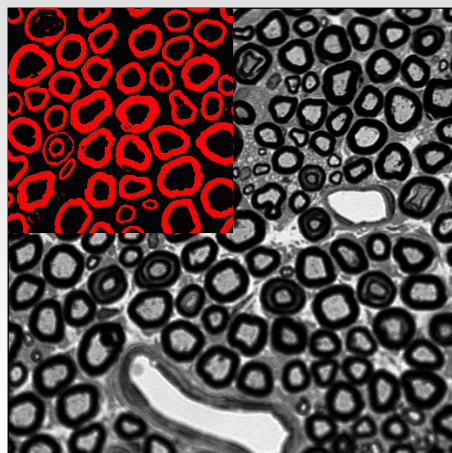
Image courtesy of J&J PRD

Ridge - Spirochetes



Spirochetes are seen with a Warthin-Starry silver stain.
inv_ridges , scale (σ) 1.0, dark ridges

Ridge - Myelin



Line detection on myelinated axon
myelin sheaths.

Sample preparation:
Toluidin blue stained, 1 μ m Epon
embedded sections

Scanning:
40x immersion oil, autofocus every 3
images

A line detector for dark ridges:
 $L_{xx}+L_{yy}-0.5*\sqrt{((L_{xx}-L_{yy})^2+4L_{xy}^2)} > 0$

Gaussian scale (σ) 1.5

Image courtesy of J&J PRD

Anisotropic Scale Space



Uneven and varying illumination conditions due to fluid in multiwell plate
Brightfield, low magnification

Anisotropic filter detects
elongated *C. elegans* nematodes

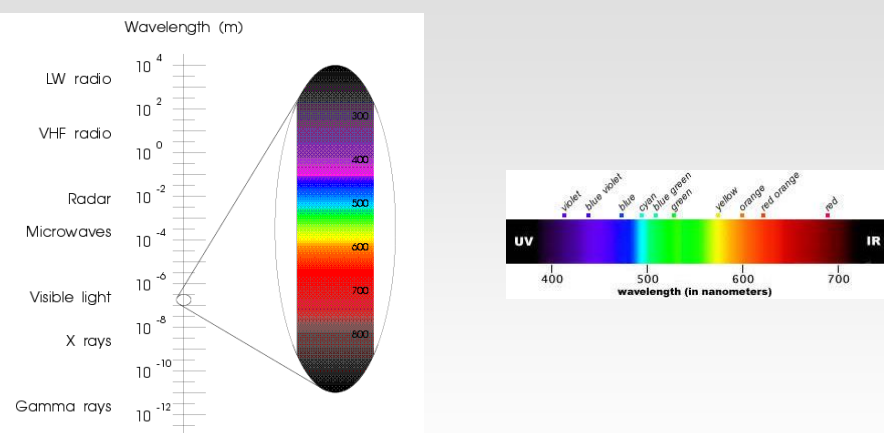
Spatial Color Model

Light and Human Vision
Light and Object
Combining Color and Spatial Extent
Robustness in applications

Light and Human Vision

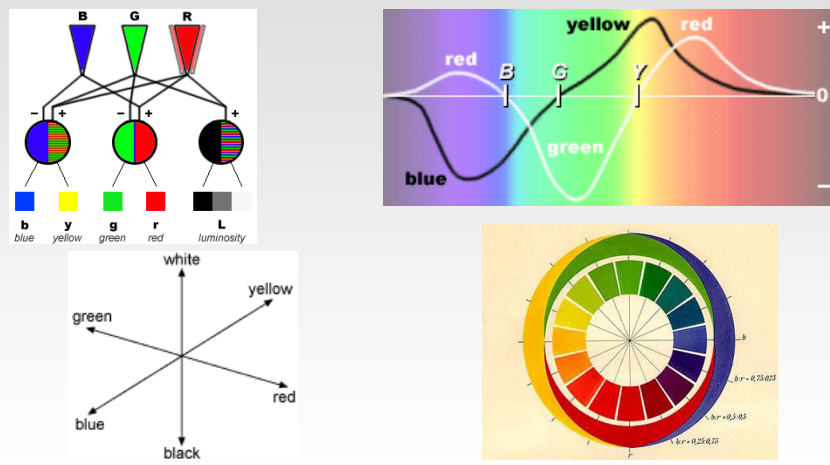
Light
Trichromatic
Opponent Color Theory

Visible Light as Electromagnetic Radiation



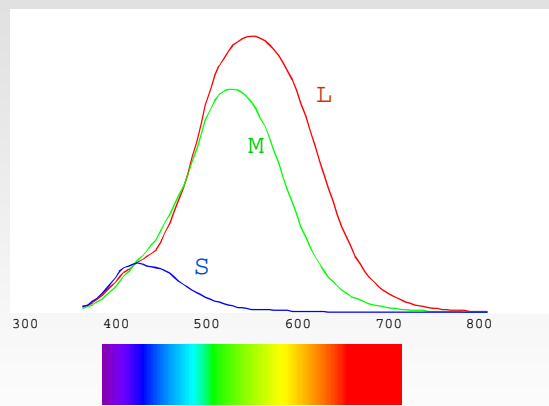
The visible light region consists of a spectrum of wavelengths, which range from approximately 700 nanometers to approximately 400 nm; that would be $7 \times 10^{-7} \text{ m}$ to $4 \times 10^{-7} \text{ m}$

Human Vision Trichromatic and Opponent Color Theory



Trichromatic theory and the opponent processing theory of color vision
Ewald Hering, Zur Lehre vom Lichtsinn, Vienna 1878

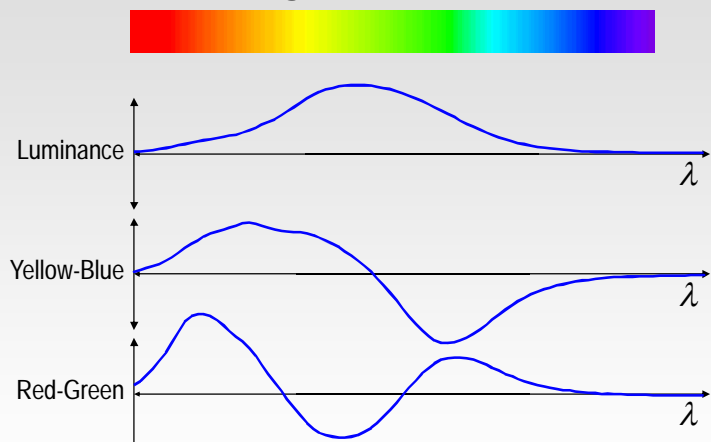
First layer of the Human Visual System Trichromatic



The cones in the retina are the fundamental units of visual information.
Long (R: 565 nm) Medium (G: 530 nm) and Short (B: 435 nm) wavelengths

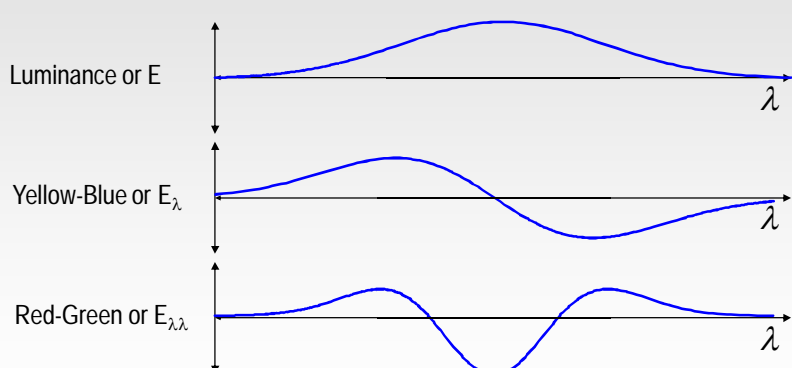
Courtesy of Jan-Mark Geusebroek

Second layer of the Human Visual System Hering Color Model



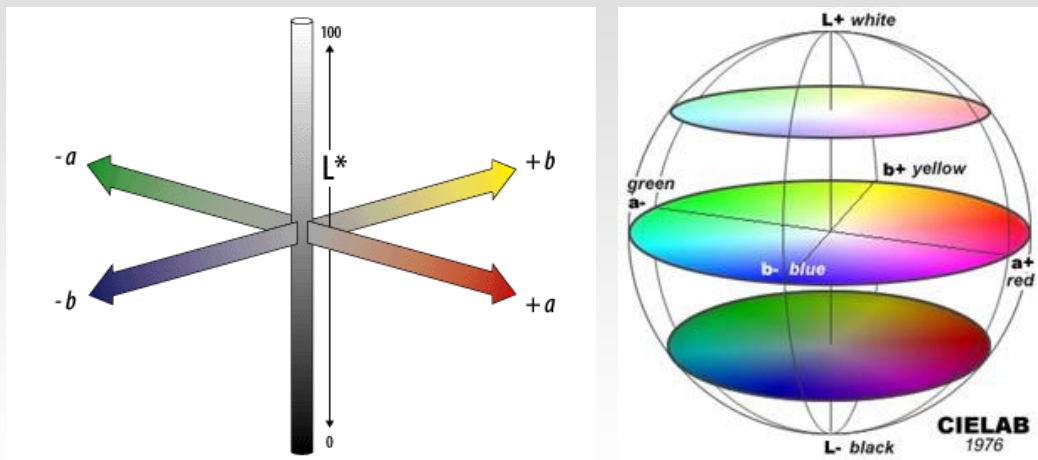
The Red Green and Blue sensitivity curves are **not** orthogonal.
Orthogonalization leads to the graphs shown here.

Gaussian Color Model



The visible spectrum (wavelength λ) is probed with a Gaussian kernel, λ_0 centered on 520 nm and width λ_σ 55.0.

CIELAB Color Model

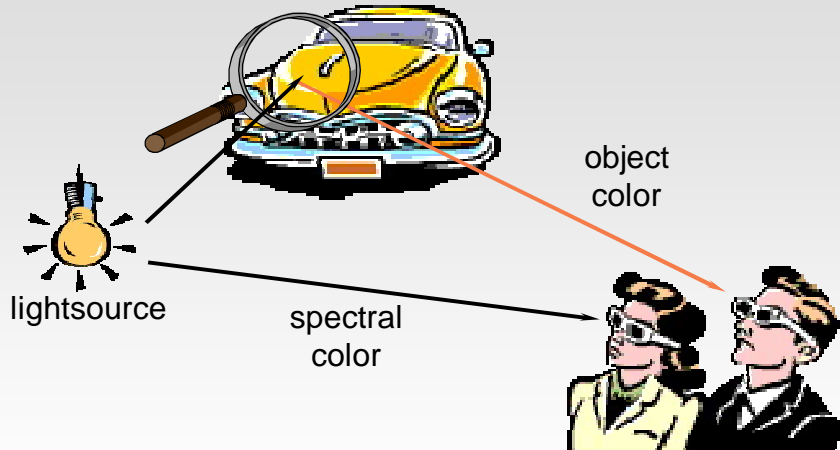


Lab in the CIELAB color model refer to analogs of the three Hering opponent process dimensions
L* is the luminosity dimension, a* is the red-green contrast, b* is the yellow-blue contrast

Light and Object

Lightsource
Interaction with Object
Highlights and Shading

The Photometric Reflection Model and Color Invariance



The Influence of the lightsource, object shading and highlights.

The object's shape (geometric information) and reflectance properties (photometric information).

Kubelka-Munk theory describing the optical property of a turbid medium which absorbs and scatters light
Fresnel reflectance of smooth surfaces, Lambertian reflection or diffuse reflection, Shafer's dichromatic reflection model

J. M. Geusebroek, R. van den Boomgaard, A. W. M. Smeulders, and H. Geerts. Color invariance. IEEE Trans. Pattern Anal. Machine Intell., 23(12):1338-1350, 2001.

Courtesy of Jan-Mark Geusebroek

Photometric reflection model

$$E(\lambda, x) = m(x)l(\lambda, x)c(\lambda, x)$$

assumption:

$$l(\lambda, x) = l(\lambda)$$

differentiation ($E = m \mid c$):

$$\frac{\partial E}{\partial \lambda} = mc \frac{\partial l}{\partial \lambda} + ml \frac{\partial c}{\partial \lambda}$$

normalization:

$$\frac{1}{E} \frac{\partial E}{\partial \lambda} = \frac{1}{l} \frac{\partial l}{\partial \lambda} + \frac{1}{c} \frac{\partial c}{\partial \lambda}$$

and thus:

$$\frac{\partial}{\partial x} \left\{ \frac{1}{E} \frac{\partial E}{\partial \lambda} \right\} = \frac{1}{c} \frac{\partial^2 c}{\partial \lambda \partial x} - \frac{1}{c^2} \frac{\partial c}{\partial \lambda} \frac{\partial c}{\partial x}$$

Courtesy of Jan-Mark Geusebroek

Object Reflectance Edge Detector

$$\begin{aligned}
 \frac{\partial}{\partial x} \left\{ \frac{1}{E} \frac{\partial E}{\partial \lambda} \right\} &= \frac{\partial}{\partial x} \left\{ \frac{E_\lambda}{E} \right\} \\
 &= \frac{E_{\lambda x} E - E_\lambda E_x}{E^2}
 \end{aligned}$$

Courtesy of Jan-Mark Geusebroek

Hierarchy of Invariants

	Illumination Intensity	Shadow	Highlights	Illumination Color
H	+	+	+	-
N	+	+	-	+
C	+	+	-	-
W	+	-	-	-
E	-	-	-	-

- H is related to the Hue
- N describes object reflectance independent of the illumination
- C describes object color regardless intensity
- W determines changes in object reflectance independent of illumination intensity

Hierarchy of invariants within the Kubelka-Munk model:

$$H \subset N = U \subset C \subset W \subset E$$

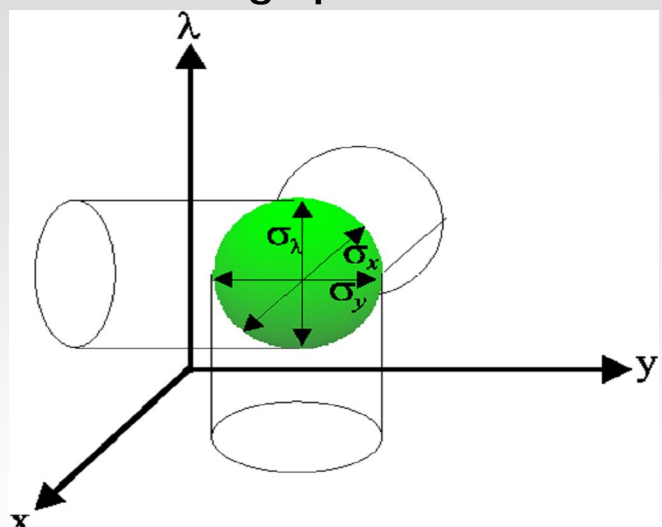
J. M. Geusebroek, R. van den Boomgaard, A. W. M. Smeulders, and H. Geerts. Color invariance. IEEE Trans. Pattern Anal. Machine Intell., 23(12):1338-1350, 2001.

Courtesy of Jan-Mark Geusebroek

Spatial Color

Color Edges
Color Patches

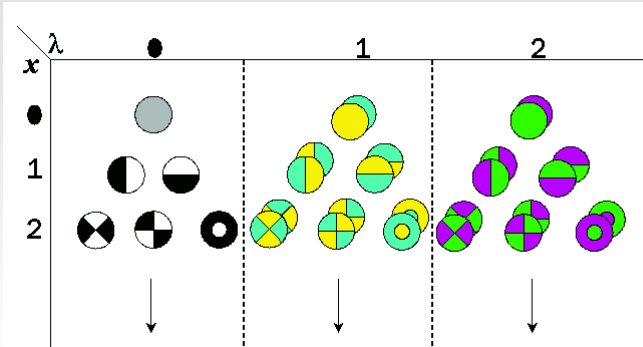
Probing Spatial Color



Spectral measurement by a physical device without knowledge about the environment

Courtesy of Jan-Mark Geusebroek

Combining Color and Space

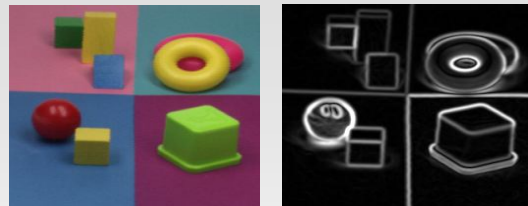


Color differentiation up to the second order, combined with Gaussian Scale Space
Integration over spectral and spatial dimensions.

Courtesy of Jan-Mark Geusebroek

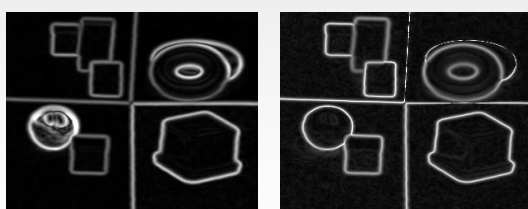
Color Transitions

Color Edge Detectors



Scene with shades and highlights

Sensitive for shading and highlights



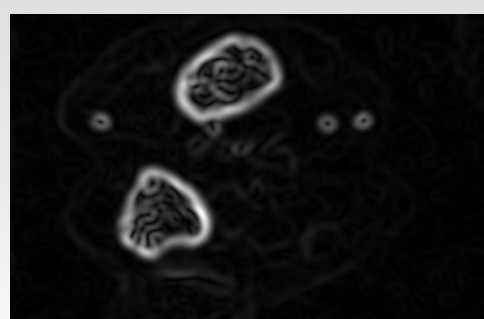
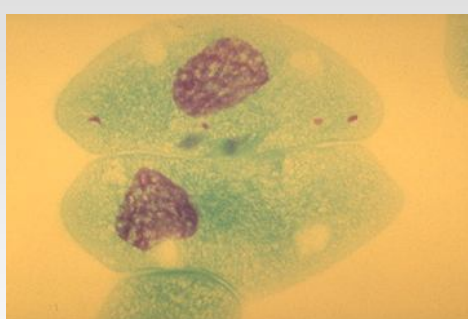
Shading invariant

Shading and highlight invariant

Detecting color edges (gradient magnitude) with increasing invariance for shading and highlights and finally only the object properties.

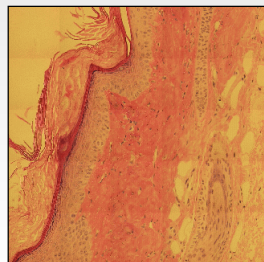
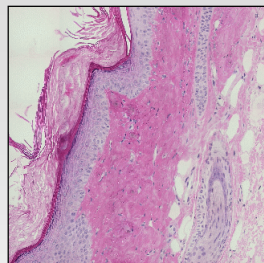
Courtesy of Jan-Mark Geusebroek

Spatial Color Model - Feulgen stain



Paramecium caudatum, Feulgen and Fast green stain
Color canny, red-green normalized edges, scale (σ) 3

Spatial Color Model and Tracing Color Edges

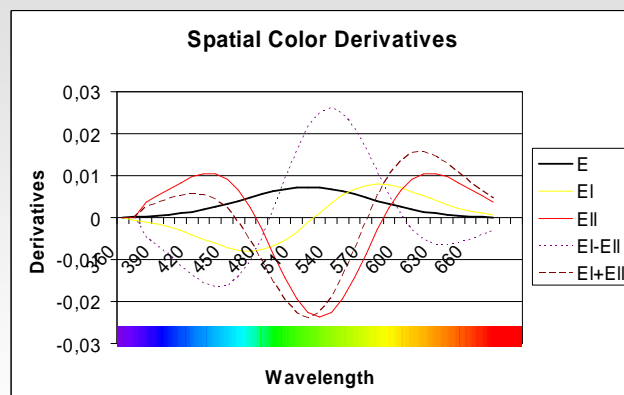


An example of color invariant edge detection. Influence of illumination color temperature on edge strength, scale (σ) is 3.0 . Skin tissue section illuminated by a halogen bulb at 4000K (top) and 2600K (bottom) color temperature.

Pictures courtesy of J&J PRD

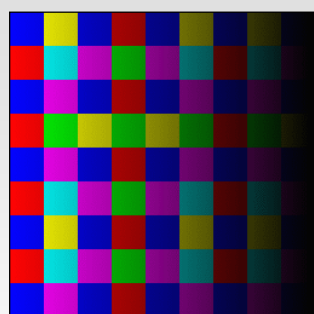
Color Patches

Selecting Color

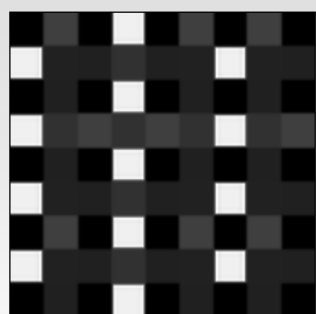


Color selection with up to 2nd order spectral derivatives to wavelength (λ).
E is luminance, EI is yellow-blue and EII is red-green

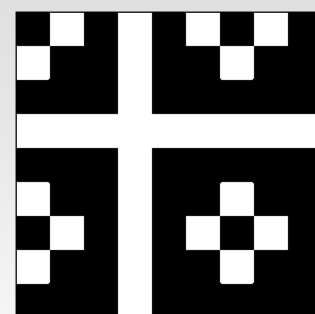
Selecting Colors Color Intensity Invariance



Color grid with intensity gradient



E_λ response '+' on yellow '-' on blue

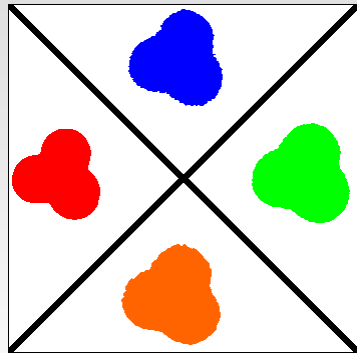
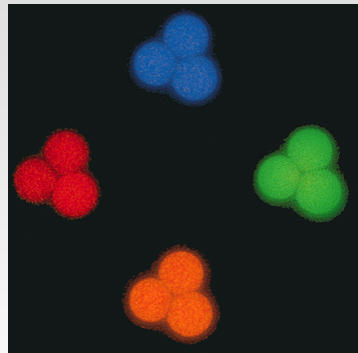


$E_\lambda > 0$ on yellow (red and green)

Detection of color regions in images.

$E_\lambda > 0$, zero crossing intensity invariance
intra- and inter scene illumination intensity changes

Spatial Color Model in Fluorescence Microscopy



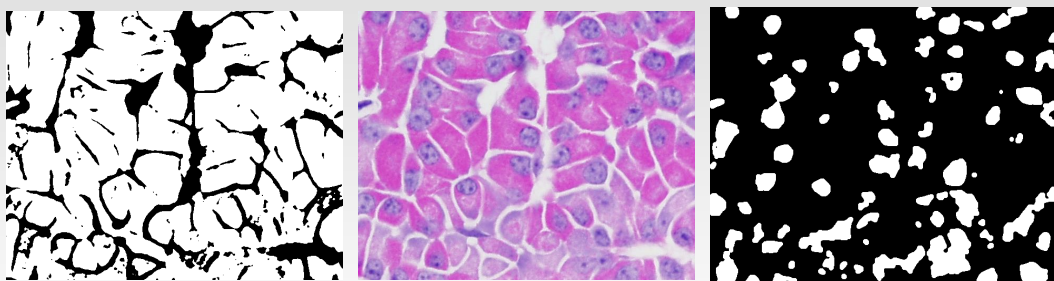
Red: $E_\lambda > 0, E_{\lambda\lambda} > 0, E_\lambda - E_{\lambda\lambda} < 0$ Green: $E_\lambda > 0, E_{\lambda\lambda} < 0$

Blue: $E_\lambda < 0, E_{\lambda\lambda} - E_\lambda > 0$ Orange: $E_\lambda > 0, E_{\lambda\lambda} > 0, E_\lambda - E_{\lambda\lambda} > 0$

Scale (σ) 1.0

TetraSpeck 4.0 μm beads photographed using optical filter sets appropriate for DAPI, fluorescein, rhodamine and Texas Red dye.

Spatial Color Model – Hematoxylin Eosin stain

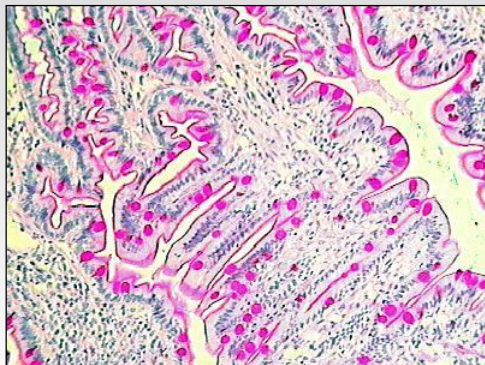


Pituitary gland, sheep, adenohypophysis 40x

Cell: $E_\lambda < 0, E_{\lambda\lambda} > 0$, scale σ 1.0

Nuclei: $E_\lambda < 0, E_{\lambda\lambda} > 0, E_\lambda + E_{\lambda\lambda} < 0$, scale σ 3.0
additional constraint added to refine selection

Spatial Color Model - PAS stain



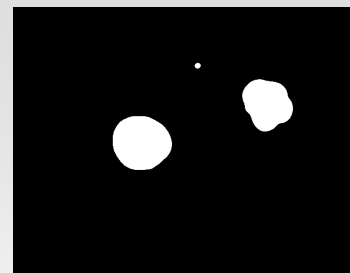
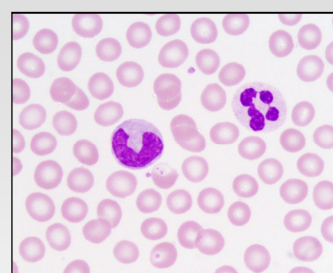
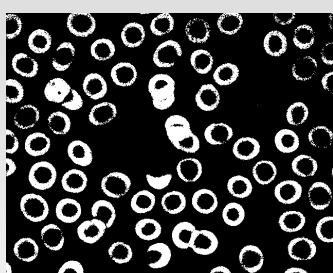
$$L_{ww} > 0, L_{vv}L_{ww} - L_{vv}^2 > 0, E_{\lambda\lambda} - E_\lambda > 0$$

Scale (σ) 2.0

P.A.S. stain for carbohydrates (goblet cells, gut)
carbohydrates stain magenta - elliptic patches

P. van Osta, J.M. Geusebroek, K. Ver Donck, L. Bols, J. Geysen, and B. M. ter Haar Romeny. The principles of scale space applied to structure and colour in light microscopy. Proc. R. Microsc. Soc., 37(3):161-166, 2002.

Spatial Color Model - Blood Smear



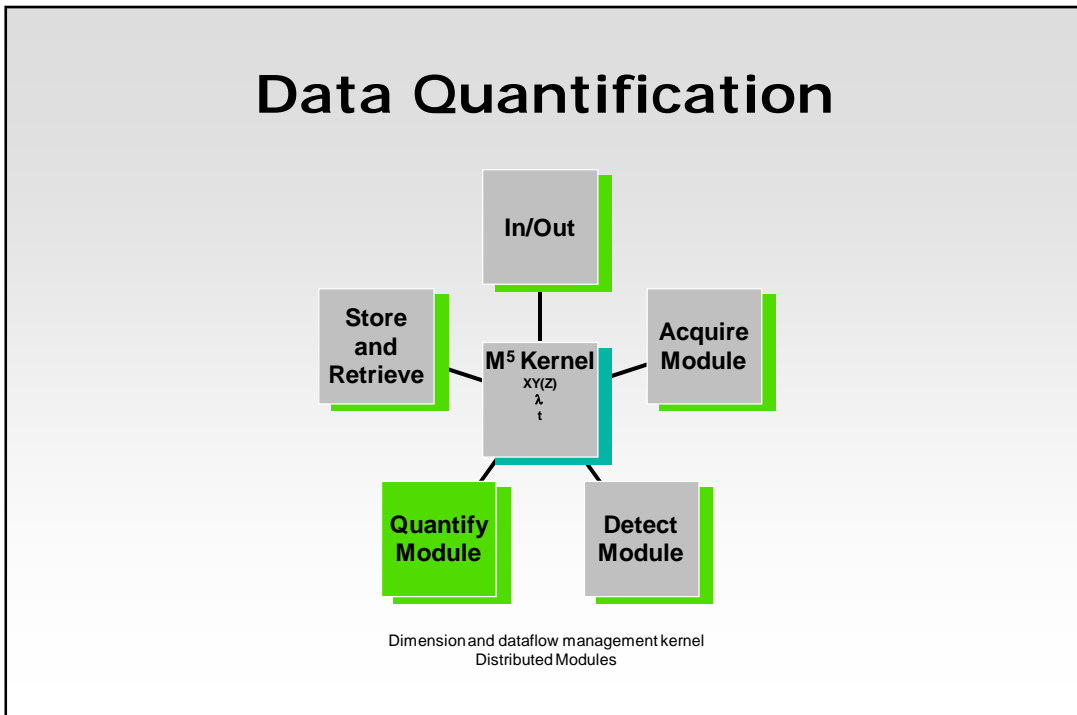
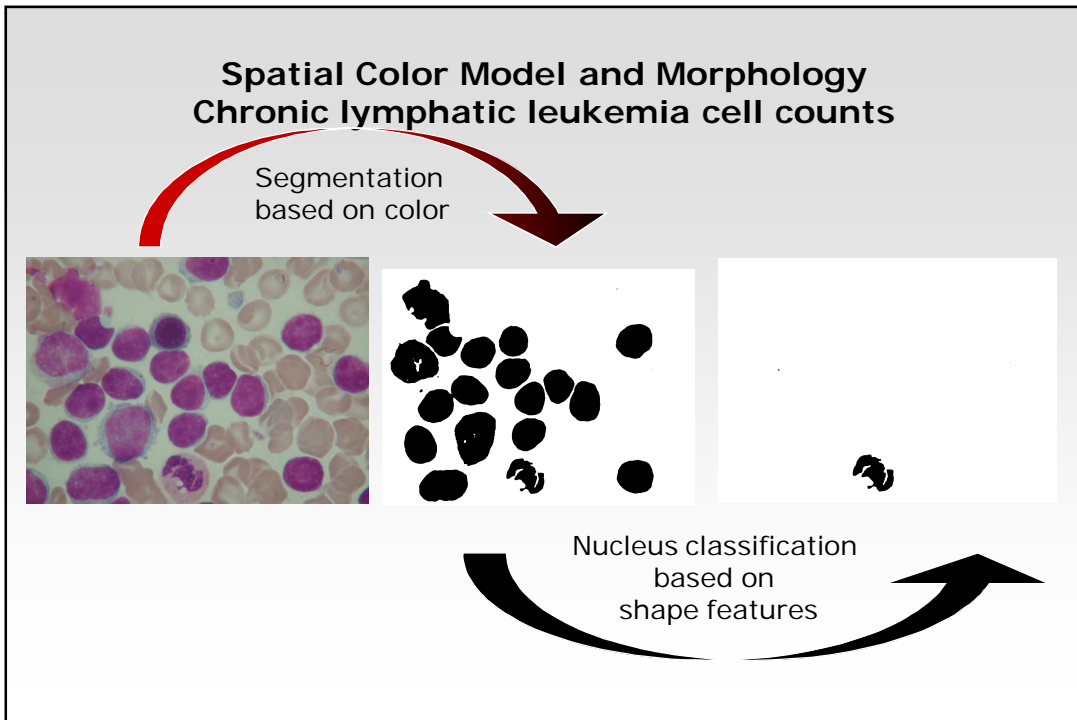
Blood smear, Giemsa stain, 100x

JPEG compression

RBC: $E_\lambda > 0$, $E_\lambda + E_{\lambda\lambda} > 0$, scale (σ) 0.5

Leucocytes: $E_\lambda < 0$, scale (σ) 12

Leucocyte nuclei: $E_\lambda < 0$, $E_{\lambda\lambda} > 0$, scale (σ) 3



Object Quantification

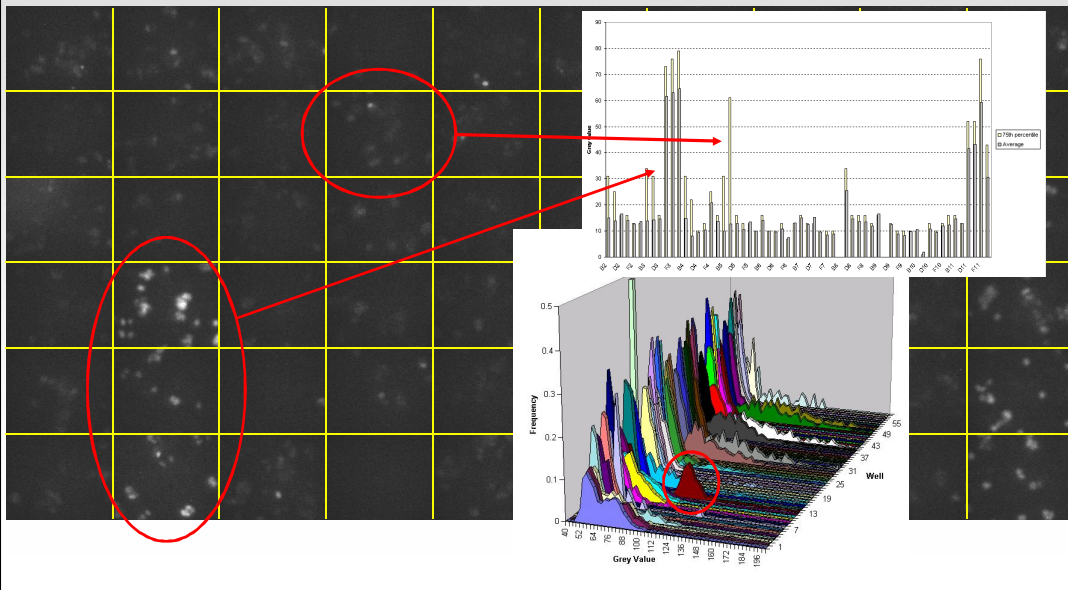
From object to number – numerical data for each object

Measurement Data Report

Object	Area	Perimeter	Contour ratio	Grey mean
1	433	89.66	1.22	169.86
2	185	54.02	1.12	178.29
3	658	94.34	1.04	204.62
4	434	76.03	1.03	216.33
5	477	82.81	1.07	211.14
6	285	60.56	1.01	203.29
7	81	32.16	1.01	160.48
8	278	61.85	1.05	173.85
9	231	53.99	1	187.47
10	30	29.14	1.5	146.2
11	501	80.11	1.01	188.14
12	660	94.08	1.03	170.7
13	99	35.34	1	164.25
14	226	54.34	1.02	194.89
15	448	75.81	1.01	208.04

Detailed intensity and morphological measurements, export to S-Plus, SAS, Excel,

Detailed data export Nuclear Expression Readout & data analysis



Overview

- Framework designed for automated research
- Extended tiled image acquisition
- Object detection
- Individual object quantification

Conclusion

- Framework designed for automated research
 - Explore space, spectrum and time
 - Distributed system for processing sample from image to data
 - Applications in cytometry, tissue morphology and model organisms
- Automated image acquisition
 - Superimages of arbitrary patterns
 - Wide magnification range (1x, ..., 40x, 63x)
 - Robust real-time automatic focus algorithm
 - Combine space, spectrum and time at different scales
- Object detection
 - Robust object shape detection
 - Scale space
 - Robust object color detection
 - Spatial color model
- Object quantification
 - Individual objects

**Union Biometrica N.V.
European Scientific Operations**
Cipalstraat 3, B-2440 Geel, Belgium

www.unionbio-eu.com
info@unionbio-eu.com

- | | |
|---------------------|------------------|
| • Johan Geysen | • Kris Ver Donck |
| • Bill Staffopoulos | • Marc Moeremans |
| • Luc Bols | • Leen Geuens |
| • Peter Van Osta | • Bieke Govaerts |
| • Bart Vanherck | |

References

- P. van Osta, J.M. Geusebroek, K. Ver Donck, L. Bols, J. Geysen, and B. M. ter Haar Romeny, The principles of scale space applied to structure and colour in light microscopy, Proc. R. Microsc. Soc., 37(3):161-166, 2002.
- J. M. Geusebroek, R. van den Boomgaard, A. W. M. Smeulders, and H. Geerts, Color invariance, IEEE Trans. Pattern Anal. Machine Intell., 23(12):1338-1350, 2001.
- J. M. Geusebroek, F. Cornelissen, A. W. M. Smeulders, and H. Geerts., Robust autofocusing in microscopy, Cytometry, 36(1):1-9, 2000.
- J.J. Koenderink, The structure of images, Biol. Cybern. 50, 363-370, 1984